NANO LETTERS

2007
Vol. 7, No. 12
3845−3848

Periodic Organic Nanodot Patterns for Optical Memory

Stephan Rath, Mark Heilig, Helmut Port, and Jörg Wrachtrup*

Physikalisches Institut, Universität Stuttgart, Pfaffenwaldring 57, 70550 Stuttgart, Germany

Received October 9, 2007; Revised Manuscript Received October 29, 2007

ABSTRACT

The fabrication of organic nanodots from photoswitchable fulgide molecules is shown. The dots are formed by dewetting of thin precursor films of the organic molecules on topographically structured substrates. In this way, we are able to control size, density, and arrangement of nanodots on millimeter-squared sized areas. We show that nanodots can be switched between isomeric molecular conformation reversibly.

The primary attraction of organic molecular nanostructures is their potential low cost and the extreme flexibility that the device engineer has in choosing a material whose properties have been specifically tailored to meet the needs of a particular application. Yet, controlled nanostructuring of organic matter while retaining its function or even creating new functionality is still under deveelopment. Dewetting of thin organic films, as shown for PS[1−5] and for small organic molecules[6,7] is a successful route toward structuring organic matter with good homogeneity over large areas. The influence of patterned substrates on the dewetting process has been analyzed and used for chemical patterning of surfaces with areas of different wettability.[8−10] Topographic patterning via substrate steps,[11] zigzag,[12] and groove[13] patterns influences the dewetting of polymer films. In this work, periodic dot patterns are fabricated by dewetting of a thin organic film from a small sized molecular photochromic compound (phenyl−thiophen−fulgide (Ph−T−F)[14] and furyl−adamantyliden-fulgide (F−Ad−F) with film thicknesses h from 2 to 22 nm). As substrate material two-dimensional periodic topographic templates are used (cylindric holes and pillars of diameters d = 420, 210, 100, and 50 nm, respectively, in hexagonal arrangement with periods of D = 800, 400, 200, and 100 nm, respectively, Etching depth is varied from 55 to 72 nm (x-lith GmbH, Ulm)). To fabricate nanodots, thin organic films are deposited at ultrahigh-vacuum conditions on helium-cooled substrates. Controlled annealing to room-temperature transforms these films into isolated dots. Various types of topographic template structures (cylindrical holes and pillars, quadratic pits, and groove patterns) have been tested. For fulgide nanodot formation, structure sizes and periods are in the range between 1700 and 50 nm. Regular dot patterns are obtained from hole and groove structures. In this contribution, we discuss dot patterns and their different possible morphologies on cylindrical holes in hexagonal densely packed arrangement. In Figure 1a, the empty substrate surface with holes of diameter d = 420 nm and period D = 800 nm is shown. Resulting dot patterns with periods of D = 800, 400, and 100 nm and with dot diameters of d = 420, 210, and 50 nm, respectivly, are displayed in Figure 1b. It should be noted that regular dot patterns are produced in millimeter-squared sized areas.

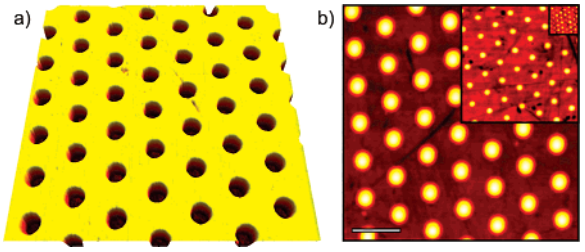

Figure 1. 5 × 5 μm AFM-scan of a glass substrate with cylindric holes in a hexagonal pattern with diameters d = 420 nm, depth h = 55 nm, and period D = 800 nm. AFM scans of periodic nanodots on hole patterns with different hole diameters. Scan sizes are 5 × 5 μm, 2.5 × 2.5 μm, and 625 × 625 nm with dot diameters d = 420, 200, and 50 nm, respectively, and periods D = 800, 400, and 100 nm, respectively. Length of white line is 1 μm. AFM topographic images have been taken ex-situ in a commercial AFM (MFP-3D by Asylum Research).

In comparison to irregular dots produced on flat substrates, the ordered dots exhibit a significantly better size homogeneity. The size distributions of dot diameter on hole pattern with d = 420, D = 800 nm are shown in Figure 2 and compared to those dots that form by dewetting on unstructured substrates. The dot homogeneity is measured by the quality factor

$$Q = \frac{\bar{d}}{\sigma}$$

* Corresponding author. E-mail: j.wrachtrup@physik.uni-stuttgart.de.

10.1021/nl072598f CCC: $37.00
Published on Web 11/17/2007

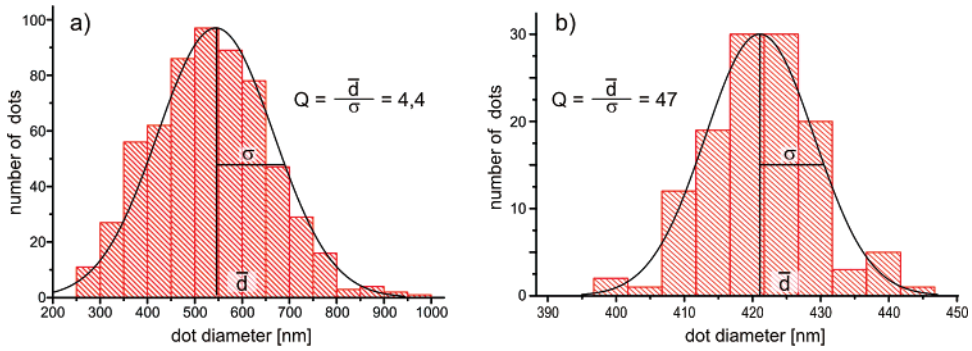

Figure 2. Size statistics of (a) dot diameters and (b) dot heights of periodic dots with $d = 420$ nm and $D = 800$ nm from a 25×25 μm AFM scan.

where $\bar{d}$ is the average dot diameter and σ is the width of the dot diameter distribution. Q is about 10 times higher for dots on structured substrates than for those on unstructured supports. This can be easily understood when considering the influence of Laplace pressure

$$p = \frac{2 \cdot \sigma_{sv}}{R}$$

of differently filled dots (R, curvature of surface and σ_{sv}, interface tension surface to vapor). Less filled dots have bigger curvature R causing smaller pressure p than more filled dots. Pressure differences equilibration results in a compensation of filling differences between neighboring dots.

In contrast to dewetting structures on unpatternd surfaces, all dots on patterns are long-term stable and do not undergo a coarsening process.

As the template structure determines the dot-position and dot-diameter, the initial film thickness h determines the dot volume. Analysis of the amount of evaporated material versus the achieved dot volumina shows in good approximation the accumulation of the complete film material in the hole pattern. Upon varying h, the amount of material accumulated in each dot can be regulated. The resulting filling degree of holes F thus can be calculated by

$$F = \frac{A_{pattern} \cdot h}{A_{hole} \cdot h_{etch}} = \frac{V_{dot}}{V_{hole}}$$

where $A_{pattern}$ is the area size of one hexagonal pattern element, A_{hole} is the cross-sectional area of holes, and h_{etch} is the etched depth of holes.

Examinations of the dewetting process on structured substrates by optical and atomic force microscopy (AFM) how that the topographic edges act as nucleation centers for the dewetting process. In competition to dewetting the material, transport by surface diffusion rearranges the molecular material. The driving motor for diffusion is the concentration gradient caused by Laplace pressure difference between droplets in wetted holes and structures on top of the substrate surface.

To get a quantitative estimate of the different dot morphologies as a function of dot filling, simulations with the software Surface Evolver[15] have been performed. In a first step, the behavior of a fluid in proximity to a topographic step has been simulated (Figure 3a).

Two principal effects can be observed:

(1) Accumulation of material in the concave edge of the step for low hole filling.

(2) Fixation (pinning) of the fluid contact line at the convex edge of the step with variable contact angle between the equilibrium contact angle θ and $\theta + 90°$ (at 90° steps).

Material accumulation can be understood qualitatively when looking at the surface and interface free energy G of such a system, which is

$$G = A_{sl} \cdot \sigma_{sl} - A_{sv} \cdot \sigma_{sv} + A_{lv} \cdot \sigma_{lv}$$

with A_{xx} the surface/interface area between phases substrate (s), liquid (l), vapor (v) and σ_{xx} the interface tension. A_{sl} and A_{sv} are of similar value for the structures used. When wetting a substrate by a fluid in the partial wetting regime, the gain or loss of free energy depends on the sizes of drop surface (A_{lv}) and drop-substrate interface. For droplets on flat surfaces always, the drop surface A_{lv} is bigger than the interface (cap shape) causing increasing energy costs with increasing such droplets. For droplets in concave edges, the wetted surface is much bigger than for comparable dots on flat surfaces, which means that these droplets have lower energy.

Pinning of the contact line can be explained by geometric considerations. At sharp edges, the fluid contact line can achieve its equilibrium contact angle by moving infinitesimal small steps around the edge.[16,17] By this the interface surface is quasi constant. Examples for such pinning effects can be found for polystyrene films on structured surfaces[18] and chemical-structured substrates with areas of different wettability.[8,9]

In a second step, the behavior of fluids in cylindrical substrate holes has been simulated and compared with experiment. As shown in Figure 3b different morphologies are obtained dependent on the filling degree F. For small F, all material is accumulated in the concave edge forming a ring-shaped filling. Upon increasing F, first pinning of the upper fluid borderline on the hole edge is observed. A further increase of F results in closed surface morphologies.

Morphological transitions can be calculated analytically for each contact angle θ by using different filling degree F

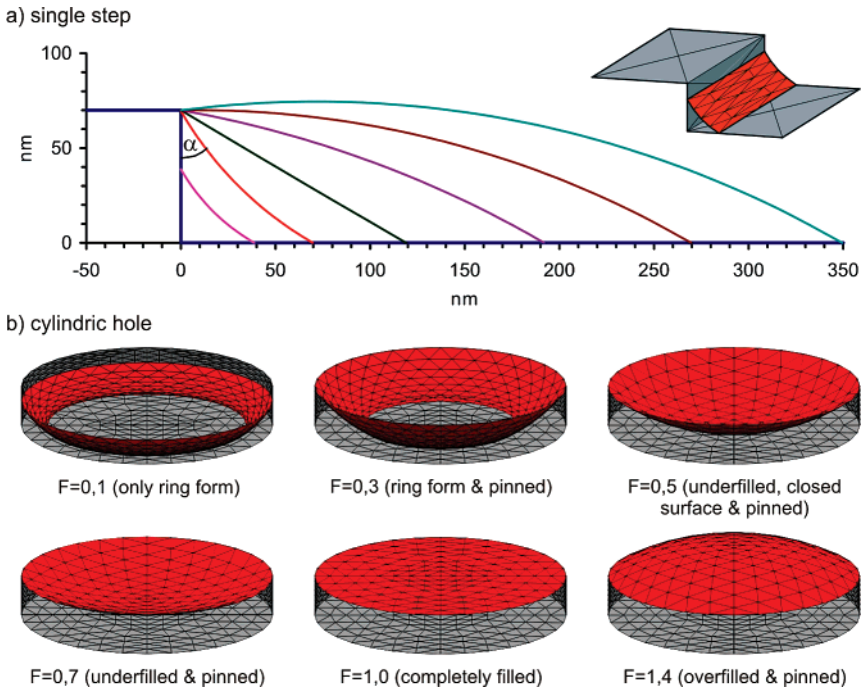

Figure 3. (a) Behavior of a fluid at a topographic step, linescans from simulated fluid surfaces (calculated with Surface Evolver[15]). Accumulation of fluid in the concave edge, pinning of the fluid borderline at the convex edge. (b) Calculations of fluid surfaces in a cylindric hole of diameter $d = 400$ nm and depth $h = 55$ nm for different filling degrees F, aspect ratio $x = h_{etcn}/d \approx 0.14$.

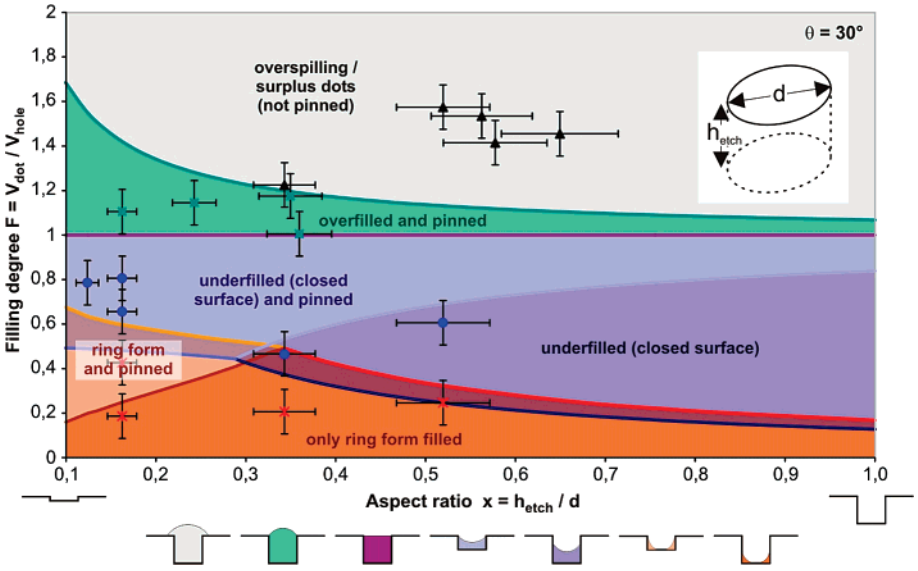

Figure 4. Calculated morphology diagram for fluid dots in cylindric holes of different aspect ratios x and filling degrees F. Measured points for filling of different hole sizes with different filling degrees. Position is defined by hole aspect ratios and evaporated material amount. Color is given by found morphology in AFM.

and hole aspect ratio $x = h_{etch}/d$, where d is the hole diameter. Results of these calculations for $\theta = 30°$, which is the equilibrium contact angle of our organic material, are shown in Figure 4. Different morphologies are shown at the bottom of this figure coded by different colors. Areas of corresponding morphologies are filled with the same color.

Dot morphologies obtained in experiments with dots of different sizes and filling degrees are marked in the morphology diagram and coded by color of the observed morphology type. Close agreement of theoretically predicted and experimentally observed filling morphologies is found. Results for different surface structures yield similar agreement between theory and experiment. We would like to stress that currently the smallest dot patterns we create have dot diameters of 50 nm with a dot spacing of 100 nm.

We apply the present structuring technique to create a fulgide-based memory device. Fulgides are photochromic molecules that undergo a conformational transition between two isomers upon absorption of UV light. The molecule used in the present experiments is a P−T−F (see Figure 5), which is switched by light of 350 nm wavelength from the E to the C isomer. The C isomer emits intense fluorescence, which

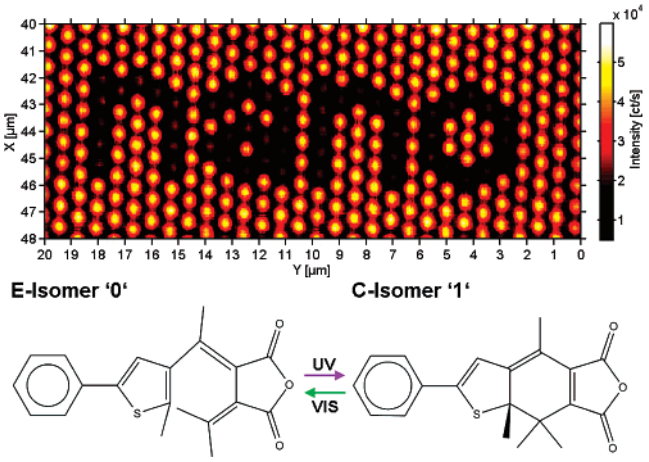

Figure 5. Data pattern "nano" stored into photochromic dot memory. Information detected by scanning an image in confocal fluorescence microscopy; bright dots store "1", dark dots store "0". Obtained on a homemade confocal microscope. Molecular structure of Phenyl-Thiophen-Fulgide (Ph−T−F). E-Isomer: 2-isopropylidene-3-[1-(2-methyl-5-phenyl-3-thienyl)ethylidene]succinic anhydride. C-Isomer: 7,7a-dihydro-4,7,7,7a-tetramethyl-2-phenylbenzo-[b]thiophene-5−6-dicarboxylic anhydride.

is used to read out the isomeric state the molecule is in. On the basis of these properties, the construction of a fulgide-based memory has been proposed.[14,19] However, while photochromic switching works for molecules in solution and for isolated molecules on surfaces it does not work in bulk molecular crystals due to steric hindrance of neighboring molecules. The small dots created however can be switched reversibly from one isomeric conformation to the other one as shown in Figure 5. Because of the regular arrangement of the dots, it is possible to calculate each individual dot position from period and orientation of the pattern. Therefore, it is possible to write binary information into whole matrices without knowledge of the prior memory state. We have to point out that due to destructive read-out (fluorescence excitation and 1−0 switching at same wavelength)[19] unlike in conventional optical memory devices, precautions to avoid loss of data have to be taken into account. One possible solution could be applying refresh procedures to stored optical information (writing of read data after reading).

In conclusion, we have created regular arrays of nanodots on millimeter-squared areas of topographic patterned substrates. In contrast to dots on unpatterned substrates, the dot arrays are long-term stable, thatis, do not undergo Ostwald ripening. We are able to predict and design dot morphologies in dependence of material contact angle, filling degree, and hole aspect ratios.

For fulgide dots, we demonstrate optical single-dot access with memory application. For the smallest dot size fabricated so far, a storage density of 74 Tbit/in^2 can be achieved that outperforms current optical storage technology by a factor of 7[20] (HD−DVD 10Tbit/in^2).

Acknowledgment. Financial support has been provided by the Deutsche Forschungsgemeinschaft DFG via the FG730 "Positioning of single nanostructures".

References

(1) Reiter, G. *Langmuir* **1993**, *9* (5), 1344−1351.
(2) Becker, J.; Grun, G.; Seemann, R.; Mantz, H.; Jacobs, K.; Mecke, K. R.; Blossey, R. *Nat. Mater.* **2003**, *2* (1), 59−63.
(3) Jacobs, K.; Herminghaus, S.; Mecke, K. R. *Langmuir* **1998**, *14* (4), 965−969.
(4) Seemann, R.; Herminghaus, S.; Jacobs, K. *Phys. Rev. Lett.* **2001**, *86* (24), 5534−5537.
(5) Sharma, A.; Khanna, R. *Phys. Rev. Lett.* **1998**, *81* (16), 3463−3466.
(6) Rath, S.; Port, H. *Chem. Phys. Lett.* **2006**, *421* (1−3), 152−156.
(7) Rath, S.; Port, H. *J. Phys. Conf.* **2007**, *61*, 981−997.
(8) Lenz, P.; Lipowsky, R. *Phys. Rev. Lett.* **1998**, *80* (9), 1920−1923.
(9) Lipowsky, R. *Interface Sci.* **2001**, *9* (1−2), 105−115.
(10) Lenz, P.; Bechinger, C.; Schafle, C.; Leiderer, P.; Lipowsky, R. *Langmuir* **2001**, *17* (25), 7814−7822.
(11) Brinkmann, M.; Blossey, R. *Eur. Phys. J. E* **2004**, *14* (1), 79−89.
(12) Rehse, N.; Wang, C.; Hund, M.; Geoghegan, M.; Magerle, R.; Krausch, G. *Eur. Phys. J. E* **2001**, *4* (1), 69−76.
(13) Seemann, R.; Brinkmann, M.; Kramer, E. J.; Lange, F. F.; Lipowsky, R. *Proc. Natl. Acad. Sci. U.S.A.* **2005**, *102* (6), 1848−1852.
(14) Rath, S.; Mager, O.; Klingler, T.; Port, H. *J. Microsc. (Oxford)* **2001**, *203*, 182−187.
(15) Brakke, K. The Surface Evolver V2.26 (Aug. 2005). http://www.susqu.edu/facstaff/b/brakke/evolver/evolver.html (accessed August 28, 2005).
(16) Gibbs, J. W. *1906 Scientific Papers*; Dover: New York, 1961; Vol. 1, p 326.
(17) Oliver, J. F.; Huh, C.; Mason, S. G. *J. Colloid Interface Sci.* **1977**, *59* (3), 568−581.
(18) Ondarcuhu, T.; Piednoir, A. *Nano Lett.* **2005**, *5* (9), 1744−1750.
(19) Rath, S.; Heilig, M.; Al-Khalisy, E.; Klingler, T.; Port, H. *J. Lumin.* **2004**, *108* (1−4), 401−405.
(20) Ohmachi, N.; Morishita, N.; Yusu, K.; Nakamura, N.; Nakai, T.; Ashida, S. *Jpn. J. Appl. Phys., Part 1* **2006**, 45 (2B), 1210−1212.

NL072598F